https://doi.org/10.5194/egusphere-2025-3127
Preprint. Discussion started: 25 July 2025

Characteristics of Legacy and Emerging Per- and Polyfluoroalkyl Substances in Atmospheric Total Suspended Particulate from The Coastal Areas in China

Shuhong Fang[1], Ximeng Zhao[1], Zhaohui Chen[1], Tingyu Yan[2], Caiqing Yan[3]

[1]College of Resources and Environment, Chengdu University of Information Technology, Chengdu 610225, China

[2]College of Electronic Engineering, Chengdu University of Information Technology, Chengdu 610225, China

[3]Environment Research Institute, Shandong University, Qingdao 266237, China

Correspondence to: Shuhong Fang (fsh@cuit.edu.cn)

https://doi.org/10.5194/egusphere-2025-3127
Preprint. Discussion started: 25 July 2025

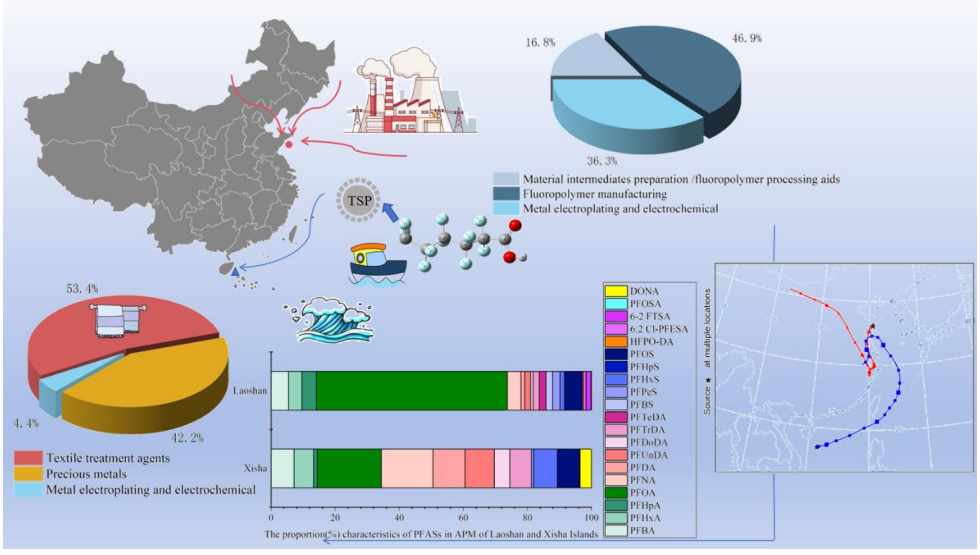

TOC/Abstract art

https://doi.org/10.5194/egusphere-2025-3127
Preprint. Discussion started: 25 July 2025

Abstract: Per- and polyfluoroalkyl substances (PFASs) could be attached to particles and transported in the atmosphere, it is necessary to investigate the characteristics of legacy and emerging PFASs in atmospheric particulates in relatively clean, low pollution open ocean in China to reveal the transport mechanism of PFASs in the atmosphere. Concentration characteristics of 30 legacy and emerging in total suspended particulate (TSP, particles with aerodynamic diameters < 100 μm) from Laoshan in Shandong and Xisha Islands in the South China Sea were analyzed. ∑PFASs in TSP ranged in 5.65 - 80.1 pg/m^3 and 3.59 -18.2 pg/m^3 for Laoshan and Xisha Islands, respectively. Generally, the long-chained PFASs were the most detected PFAS, with the detection frequency of 73.1% and 72.0%. Perfluorooctanoic acid(PFOA) were the main PFAS, with the profiles of 57.1% and 21.0%, respectively. Principal component analysis and multiple linear regression (PCA-MLR) showed that the Laoshan was dominated by fluoropolymer manufacturing (46.9%) and metal electroplating/electrochemical processes (36.3%), while the Xisha islands exhibited primary contributions from textile treatment sources(53.4%) and precious metal sources (42.2%). The backward trajectory clusters for 24 h/120 h showed that air masses in the Laoshan primarily originated from northern (23%) and southeastern (28%), the Xisha Islands were predominantly sourced from the northeastern (80%), overlapping transport paths of air masses between the two regions within the same altitude range. This suggests that that the similarity of PFAS distribution characteristics between Laoshan and Xisha may be related to long-distance atmospheric transport between the two regions.

Keywords: Per- and Polyfluoroalkyl substances, Total suspended particulate (TSP), Coastal area in China, Source apportionment, Long-distance transport

https://doi.org/10.5194/egusphere-2025-3127
Preprint. Discussion started: 25 July 2025

1. Introduction

Per- and polyfluoroalkyl substances (PFASs) are a large group of synthetic organic chemicals and have been widely used in the chemical industry, leather, medicine, and other industrial and commercial fields (Prevedouros et al., 2006) for more than 6 decades. They have been widely detected in the atmosphere (Zhang et al., 2020), water (Li et al., 2022), soil (Wang et al., 2018), wildlife (Schuetze et al., 2010) and human tissues (Kannan et al., 2004) in recent years. Previous studies have proved that PFASs have endocrine toxicity, carcinogenicity, neurotoxicity, and reproductive toxicity, and have potential risks to the environment and organisms (Yu et al., 2018b). Therefore, PFOS and PFOA, which are commonly detected in environment, were listed in the Stockholm Convention in 2009 and 2019, respectively (UNEP, 2019).

Then, the short-chain and emerging PFASs have been applied in the market as alternatives. Hexafluoropropylene oxide dimer acid (HFPO-DA, also called GenX) has been produced and used in the production of fluoropolymer high performance materials as a substitute for PFOA(Wang et al., 2013). Chlorinated polyfluorinated ether sulfonate (Cl-PFESA) has been used to replace PFOS in mist suppressants in the metal plating industry (Wang et al., 2014). The emissions of PFASs alternatives have increased significantly in recent years (Zhang et al, 2020), and the research results show that these substitutes have certain bioamplification and bioaccumulation effects (Deng et al., 2018) and toxicity (Li et al, 2018;Sheng et al, 2017), which has aroused public concern. Therefore, studies focusing on the short-chain and emerging PFASs substitutes are needed.

As is known to all, organic pollutants in the atmosphere have adverse effects on human health in direct, and respiration is one of the main exposure routes of PFASs (Liu et al., 2017). To date, few studies have focused on atmospheric PFASs in China. PFASs can enter to atmosphere by volatility from water and soils in areas, and then subject to long distances atmospheric transport to remote areas (Stock et al., 2004; Wang et al., 2018). The ocean and atmosphere frequently exchange matter and energy, forming a highly complex coupling system. At present, PFASs have been detected at varying concentrations worldwide, including in atmospheric samples from Japan's northwestern coast (Piekarz et al., 2007), marine waters and coastal urban areas of China (Fang et al., 2018; Yao et al., 2017), and Europe's Mediterranean region (Jahnke et al., 2007). Atmospheric suspended particles often serve as carriers for perfluoroalkyl and polyfluoroalkyl substances (PFASs), which are adsorbed onto these particles through van der Waals forces and coordination reactions (Weinberg et al, 2011;Piekarz et al, 2007). Oceanic processes (waves, storms, and biogenic activity) generate suspended sea-salt aerosols and organic particulates (Gemma et al., 2020), which interact with atmospheric $PM_{2.5}$/PM_{10} to transport PFAS. Thus, as a critical source-sink interface, the ocean accelerates PFAS exchange between marine and atmospheric systems, participating in global atmospheric circulation and altering atmospheric chemical composition and physical properties. However, current studies predominantly focus on PFAS occurrence characteristics and source apportionment within single regions, while long-range transregional transport mechanisms remain insufficiently explored.

In this study, 30 legacy and emerging PFASs were quantified in atmosphere TSP samples of Laoshan and Xisha Islands. The objectives of this study are to: (1) investigate the occurrence and composition of legacy and emerging PFAS in atmosphere samples from Laoshan and Xisha Islands; (2) identify the sources of PFAS using principal component analysis and multiple linear regression(PCA-MLR) model; (3) The backward trajectory (HYSPLIT) model was used to investigate the source trajectory of PFASs in the atmosphere of Laoshan Mountain and Xisha Islands and whether it has long-distance transport behavior. Monitoring legacy and emerging PFAS in the air and has important implications for the

https://doi.org/10.5194/egusphere-2025-3127
Preprint. Discussion started: 25 July 2025

development of pollutant abatement measures taken by policy makers in the study area.

2. Materials and methods

2.1. Sample collection

Tisch-TE 5170 high-flow atmospheric comprehensive sampler and quartz membrane were used for sampling. Before sampling, all the quartz fiberfilters (PALLFLEX Membrane Filters, 250 mm×200 mm, TISSUQUARTZ-2500QAT-UP) were calcined for 4.5 h in a muffle furnace at 550℃. In March 2021, atmospheric suspended particulate matter was sampled in the Xisha Islands with 12 h at day and 12 h at night, with a total of 23 samples. From 16th April to 16th May in 2021, a total of 26 atmospheric samples were collected in Laoshan, Shandong Province for one consecutive month. The sampling sites were showed in Fig.1. Each sample was conducted for nearly 12h or 24 h at a flow rate of 40 L min^{-1}. The sampled quartz membrane was folded, wrapped in aluminum foil, and placed in a sealed PP bag. Samples were preprocessed immediately after returning to the laboratory, and the pretreated samples were stored at 4 ℃ until analysis. Details regarding the sampling campaign are provided in Table S1-S2.

2.2. Reagents, extraction, and analyses

Methanol (HPLC grade, 99.9%, Chengdu Kelon Chemical Reagent Factory, China), ammonia water (25%, Chengdu Kelon Chemical Reagent Factory, China), acetic acid (analytical reagent, purity:>99.5%) and ammonium acetate (HPLC grade, purity>98.0%) was purchased from Chengdu Kelon Chemical Reagent Factory. The standard sample used in the experiment is high purity mixed standard PFAC-MXB (Wellington laboratories, Guelph, ON, Canada), including 11 perfluoroalkyl carboxylic acids (PFCAs), 7 perfluoroalkyl sulfonic acids (PFSAs), 3 n:2 FTSs, 2 n:2 Cl-PFESAs, FOSA, FBSA, FHxSA, HFPO-DA, N-MeFOSAA, N-EtFOSAA, and ADONA. MPFAC-MXA used in this study is a 19-mixed high-purity internal standard (Wellington laboratories, Guelph, ON, Canada). Details regarding the standards are provided in Table S3.

The detalis for sample preparation was provided in Text S1. Briefly, quartz membranes were extracted twice with methanol in an ultrasonic bath. The two methanol extracts were combined, evaporatedto 5 mL under a gentle stream of dry nitrogen gas and thenwere purified by Cleanert PestiCarb SPE cartridges (Bonna-Angla Technologies, China). The final concentrated extract was filtered through a 0.22 μm nylonfilter and transferred into an injection vial, and finally stored at 4 °C for analysis.

PFASs were confirmed and quantified using an ultra-high performance liquid chromatography tandem triple quadrupole mass spectrometer instrument (Agilent, 1290-6470) fitted with a C18 chromatographic column (Zorbax SB-C18, 2.1 mm × 50 mm, 1.8 μm). The mass spectrometer was operated in the negative electrospray ionization with multiple reaction monitoring (MRM). Details regarding UPLC MS/MS analysis parameters are provided in Text S2.

2.3. Quality assurance and quality control (QA/QC)

To reduce the experimental background, all samples were avoided to contact Teflon containers during the pretreatment process. The standard calibtation curve samples were 0, 0.05, 0.1, 0.5, 1, 2, 5, 10, 20 and 50 ng/mL with the linear relationship $R^2 > 0.99$. All target analytes were quantified using an internal standard except for 6:2 Cl-PFESA, 8:2 Cl-PFESA, HFPO-DA, and ADONA. In order to monitor

https://doi.org/10.5194/egusphere-2025-3127
Preprint. Discussion started: 25 July 2025

any process contamination, a total of three field blanks were sampled and two procedural blanks were set for each batch of 10 actual samples that were analyzed for target PFASs. To monitor the instrument background, methanol was injected after each batch of 12 samples as solvent blank and analyzed with the same instrumental method as the actual samples. The PFAAs were not detected in all the blank samples or were below their corresponding MDLs in the procedural blanks, filed blanks, and methanol.Two different concentrations (spiking levels of 2 ng and 20 ng for each PFAS) were set in the recovery experiments, with 3 replicates for each concentration level. The recoveries of all target compounds were in the range of 69.3%-128.4% (Table S4). The method detection limits (MDLs) were defined as the lowest point on the calibration curve with a signal-to-noise ratio of 3, if the specific PFASs were not detected in procedural blanks. For the compounds detected in procedural blanks, MDLs were defined as the mean blank concentration plus three times the blank standard deviation. The method detection limits of all target compounds were in the range of 0.009-0.841 pg/m^3. When calculating the total concentration, the MDL was substituted by dividing the $\sqrt{2}$ if the detected value is lower than the MDL, while it was substituted by zero when not detected.

2.4. Statistical analysis

Spearman correlation analysis was carried out to examin correlation between different PFASs, principal component analysis and multiple linear regression (PCA-MLR) were implemented to analyzing pollution sources of PFASs. All data analysis charts such as concentrations and components were performed using the Origin 2019b software (USA). The spatial distributions map of the sampling sites was illustrated using the ArcGIS 10.7 (USA).

2.5. Backward Trajectory and source apportionment

The hybrid single-particle Lagrangian integrated trajectory model (HYSPLIT, Version 4, Air Resources Laboratory) was used for backward trajectory analysis, and the PCA-MLR model was used to reduce the dimensionality of the data through principal component analysis, and factors with eigenvalues greater than 1 were selected as principal components. The source of pollution is inferred according to the load of the principal component on each pollutant, the load greater than 0.8 is selected as the main pollutant for source analysis. Multiple linear regression analysis was used to obtain the average contribution rate of each pollution source, and the potential sources of perfluorinated compounds in suspended particulates were predicted (Cohen et al., 2015).

The back trajectory of the air mass reaching 500 m above the surface was analyzed at intervals of 24 hours and 120 hours respectively. (Wang et al., 2017). Before treating large variations in total spatial variance (TSV) as clusters of trajectories, wind direction and speed are added to the clusters based on the geometric distances corresponding to individual trajectories. The MLR model equation is as Eq.(1), the formula for calculating the average contribution rate is as Eq.(2) (Thurston & Spengler, 1985):

$$y = \sum_{i=1}^{p} B_i X_i \quad (1)$$

$$Z = \frac{B_i}{\sum B_i} \times 100\% \quad (2)$$

Where y is the total concentration of PFASs, p is the number of principal components, B_i is the multiple linear regression coefficients, X_i is the factor score of the principal component, Z is the average contribution rate of the source i.

https://doi.org/10.5194/egusphere-2025-3127
Preprint. Discussion started: 25 July 2025

3. Results and discussion

3.1. Concentrations and profiles of PFASs in APM of Laoshan

Nineteen per- and polyfluoroalkyl substances were detected in the atmospheric samples of Laoshan. Legacy PFASs including PFHxS, PFOA, PFOS, PFNA, and PFUnDA were detected in all samples, followed by PFHxA (96.2%), PFDA (96.2%), PFDoDA (92.3%), PFHpA (88.5%), PFBA (84.6%) and the precursor PFOSA (88.5%), while PFPeA was not detected in any samples. Concentration of Σ_{19} PFASs ranged from 5.65 to 80.1 pg/m^3, with the mean and median values of 27.7 and 21.3 pg/m^3 respectively (See Fig.2. and Table S5). The main PFASs were PFOA、PFBA、PFHxA and PFOS. The concentration was the highest on April 19th and the lowest on May 9th. The wind direction on April 19 was southwest, the wind speed was 4.3 m/s, and the weather was clear. On May 9th, there was rainfall and a southeast wind with a wind speed of 4.7 m/s. Under similar meteorological conditions, the rainfall scavenging exhibits enhanced efficiency in atmospheric PFAS removal compared to dry deposition.

The primary substances detected in other areas of TSP, such as Bohai Sea and Yellow Sea, were FTOH (Zhao et al, 2017), PFBS and PFOS (Billah et al, 2016). But the PFOA displayed the highest concentration (3.18-48.0 pg/m^3, mean: 16.5 pg/m^3), with the profiles of 57.1% (27.1%-83.6%) in Laoshan. This may be attributed to regional industries such as chemical manufacturing, metal plating, or textile processing, which directly release PFOA into the atmosphere. In general, the levels of PFOA in Laoshan APM were slightly higher than in China Nanjing (11.6 pg/m^3), Beijing (12.5 pg/m^3), Guiyang (2.07 pg/m^3), Shenzhen (15 pg/m^3), Guangzhou (11.7 pg/m^3) and Yancheng (8.3 pg/m^3) (Yu et al., 2018a). In addition, Kjeller (Norway, 1.54 pg/m^3), Mace Head (Ireland, 8.9 pg/m^3) (Barber et al., 2007), Geesthacht (Germany, 0.7 pg/m^3) (Dreyer et al., 2015) and Toronto(Canada, 0.01 pg/m^3) (Ahrens et al., 2012) also displayed lower PFOA concentrations than Laoshan. The levels of PFOA in Laoshan were lower than in Qingdao China (73.8 pg/m^3), Jinan (China, 325 pg/m^3) and Yantai (China, 30.7 pg/m^3), as well as Oyamazaki in Japan (267.2 pg/m^3) (Harada et al., 2005), Hazelrigg (552 pg/m^3) and Manchester (341 pg/m^3) in the UK (Barber et al., 2007).

HFPO-DA, an alternative of PFOA, has been found in TSP in Laoshan, with the concentration and detection frequency of nd.-0.95 pg/m^3 and 38.5%. Some studies have found that when HFPO-DA meets·OH, oxidation reaction may occur, resulting in the break of some chemical bonds in the molecule, which making it difficult to exist stably in the atmosphere for a long time. As the alternative of PFOS, 6:2 Cl-PFESA (nd.-1.12 pg/m^3) and 6:2 FTSA (nd.-3.07 pg/m^3) were both detected in the atmospheric samples, with the detection frequencies of 30.7% and 80.6% respectively. The concentration of Cl-PFESA detected in particulate matter in the air in Dalian ranges of 85.9 to 722 pg/m^3, which is significantly related to the large number of electroplating industrial areas in the region, and also indicates the widespread use of emerging PFAS in China (Liu et al, 2017).

It was worth noting that the long-chain PFCAs(C_8-C_{14}) accounted for the largest proportion (73.1%, mean value) in Laoshan atmosphere among which PFOA is the predominant substance,indicating that long-chain PFCAs were more inclined to be adsorbed by particulate matter in the atmosphere than short-chain (C_4-C_7) PFCAs and PFSAs. PFBA was the dominant short-chain PFCA with concentrations of nd.-5.56 pg/m^3, followed by PFHpA (nd.-6.62 pg/m^3).

3.2. Concentrations and profiles of PFASs in APM of Xisha Islands

The levels of PFASs in each sample of Xisha Islands were showed in Fig.3. and Table S6. Fourteen

https://doi.org/10.5194/egusphere-2025-3127
Preprint. Discussion started: 25 July 2025

PFASs were widely detected in APM samples, demonstrating the widespread of PFASs in the Xisha Islands atmosphere. PFHpA, PFOA, PFNA, PFDA, PFUnDA and PFDoDA were detected in all samples, then were PFHxA (95.7%), PFOS (95.7%), PFBA (87.0%) and PFHxS (87.0%), while PFPeA and PFBS were not detected in any samples. The total concentration of PFASs ranged from 3.59 to 18.2 pg/m^3, with the mean and median concentrations of 8.56 and 6.93 pg/m^3 respectively, which were slightly lower than Laoshan. It is due to fewer pollutions around the Xisha Islands. Same as Laoshan, PFOA (0.92-4.42 pg/m^3) was predominant with an average contribution of 21.0% (14.5%-33.1%) in Xisha Islands atmosphere samples, followed by PFNA (0.64-2.56 pg/m^3), which accounted for 17.3% (10.8%-23.7%) of $\sum_{14}$ PFASs. There were two emerging PFASs detected in APM samples from Xisha Islands. The detection frequencies of 6:2 FTSA (nd.-0.04 pg/m^3) and ADONA (nd.-4.23 pg/m^3) were 56.5% and 13%, respectively.

In general, the concentration of PFASs in the daytime was higher than at night, especially in the 14th and 16th. The light and temperature in daytimeyou are conducive to induce precursor conversion. The highest average daily concentration was on 14 days, which was mainly due to higher PFOA levels. While the concentration was slightly lower during the day such as 7th, 12th and 15th, it is speculated that the corresponding night samples during this period are collected when the ship stops, and the concentration of pollutants will be higher than the samples collected during the sailing. The daytime concentration was the highest on the 16th, and the difference between day and night concentration was significant, mainly because the day and night samples were collected when the ship was stationary and sailing. It has been confirmed that air flow rate is the key factor to affect the diffusion of pollutants in atmosphere, and higher flow rate would induce a wider diffusion range and reduce the concentration per unit volume (Qin et al., 2021). Thus, it can be inferred that the ship's operation speeds up the air flow, which could quickly carry away the pollutants around the sampling site, and play a dilution role.

As showed in Fig.S2, the L-PFCAs also accounted for a large proportion(72.0%, mean value), which also provided an evidence that long-chain PFASs were more inclined to be adsorbed by particulate matter. Overall, the proportional characteristics of the daytime were consistent with night. However, the proportion characteristics of daytime on different days changed relatively greatly, and the main difference was reflected in the detection of 6:2 FTSA and ADNOA.

The monitoring point was extended to the surrounding area, and the geographical distribution of concentrations characteristics in the area was predicted based on the detection of PFOA, PFNA, L-PFCAs and Σ14PFASs, as shown in Fig.4. Generally, the target concentration on land was higher than ocean, suggesting a influence of industrial and human activities. And it showed a increasing trend from northeast to southwest. It may be due to that the prevailing wind here is northeasterly, resulting in a higher concentration at downwind areas. PFOA showed the highest concentration levels in the northwest and the northwest of Xisha Islands, and then displayed the decreasing trend to the seat, indicating industry and human activities emission were the main sources of PFOA to TSP (Fig.4a). PFNA showed a lower concentration in the northwest, while in the northeast and southwest is higher, suggesting that PFNA in this atmosphere may not be directly affected by local industrial and human activities but long distance atmospheric transporting(Fig.4b). The levels of L-PFCAs and Σ_{14}PFASs showed a similar distribution pattern which highest concentration in northwest area(Fig.4c and 4d). The results indicated that traditional and long-chain PFASs were still the dominating PFASs.

https://doi.org/10.5194/egusphere-2025-3127
Preprint. Discussion started: 25 July 2025

3.3. Component correlation and source apportionment

The Pearson correlation coefficients were further investigated between the PFASs in APM (Table S7-S8), a significant correlation generally indicated similar sources, transport processes and transformation processes for the two components(Lai et al., 2016). Moderate to strong correlations were shown between PFCAs, suggesting that PFCAs in the atmosphere from Laoshan and Xisha Islands may originate from common sources, such as atmospheric transport. In Laoshan, PFOS showed moderate to strong correlations with PFCAs, especially PFOA ($r = 0.832$, $p = 0.000$) and PFDA ($r = 0.806$, $p = 0.000$). HFPO-DA was found to be moderately correlated with PFBA ($r = 0.588$, $p = 0.002$), PFOA ($r = 0.668$, $p = 0.000$) and PFTeDA ($r = 0.582$, $p = 0.002$), while PFOSA only showed moderate correlation with PFTrDA ($r = 0.671$, $p = 0.000$). Both 6:2 Cl-PFESA and 6:2 FTSA showed weaker and less significant correlations with others, except for 6:2 FTSA and PFBA ($r = 0.646$, $p = 0.000$). In Xisha Islands, PFOA as the predominant PFASs showed significantly positive correlations with PFHxA ($r = 0.868$, $p = 0.000$), PFNA ($r = 0.855$, $p = 0.000$), PFDA ($r = 0.906$, $p = 0.000$) and PFDoDA ($r = 0.907$, $p = 0.000$). As two alternatives to PFOA and PFOS, ADONA and 6:2 FTSA($r = 0.639$, $p = 0.001$) was found to be moderately correlated with with PFPeS($r = 0.788/0.669$, $p = 0.000$), and ADONA also showed a moderate correlation with PFHxS ($r = 0.541$, $p = 0.000$).

To explore the potential sources of PFASs in APM from the sampling regions, a principal component analysis (PCA) was applied to the factor extraction. The species with poor linear correlation and Kaiser-Meyer-Olkin (KMO) value less than 0.5 were excluded to participating in principal component analysis, and finally 13 and 12 PFASs were extracted from the three principal components of Laoshan and Xisha Islands, respectively (Table S9-S10).

In Laoshan, three principal components explain the sources of 82.6% of PFASs in the atmosphere at this sampling site. FL1 accounted for 56.7% of the total variances, among which PFUnDA and PFNA are in high loading of 0.976 and 0.930, respectively. PFUnDA was used for the preparation of material intermediates (Xiao et al., 2012); PFNA has been used for many decades as an essential “processing aid” in the manufacture of pfluoropolymers (Buck et al., 2011), thus FL1 was interpreted as the source of material intermediates preparation and fluoropolymer processing aids. FL2 explained 15.2% of the total variances and was characterized by HFPO-DA with high loading of 0.938, which was used as PFOA alternative in the fluoropolymer manufacturing industry(Wang et al., 2013). FL3 explained 10.7% of the total variances, among which PFHpS and PFOS are the marker of pollutants with loading of 0.948 and 0.801, respectively. PFOS has been widely used in the metal electroplating industry in Qingdao city(Wang et al., 2020), and the fluorine industry usually produces PFOS and other PFSAs by electrofluorination derivatization(Liu et al., 2015), therefore, FL3 was defined as the source of metal electroplating and electrochemical industry.

In Xisha Islands, three principal components explain the sources of 84.8% of PFASs in the atmosphere at this sampling site. FX1 accounted for 56.1% of the total variances, among which long-chained PFCAs, especifically PFDoDA, PFUnDA, PFOA and PFDA with high loading of 0.952, 0.895, 0.867, and 0.861, respectively. Long-chained PFCAs (C_{10}–C_{16}) were commonly used as impregnation sprays for automotive textile upholstery, thus FL1 was defined as the source of textile treatment agents(Cai et al., 2012). FX2 explained 18.8% of the total variances and was characterized by PFBA with high loading of 0.822, which was mainly used as a flotation agent in the synthesis of precious metals (Campo et al., 2015). FX3 explained 9.88% of the total variances, among which PFPeS and 6:2 FTSA are the marker of pollutants with the loading of 0.904 and 0.864, respectively. 6:2 FTSA was the main degradation product of fluorotelomer surfactants and was widely applied as alternative to PFOS in metal

https://doi.org/10.5194/egusphere-2025-3127
Preprint. Discussion started: 25 July 2025

plating(Hoke et al., 2015; Yu et al., 2018a), therefore, FX3 was defined as the source of metal electroplating and electrochemical industry, too.

Using the MLR method to regress the standardized ∑PFASs and PCA factor scores, the regression equation of Laoshan and Xisha Islands can be expressed as Eq.(5) and Eq.(6), respectively(Qi et al., 2017):

$$Z_L = 0.263FL1 + 0.736FL2 + 0.57FL3 \quad (R^2=0.935, P=0.000) \quad (5)$$

$$Z_X = 0.779FX1 + 0.615FX2 + 0.064FX3 \quad (R^2=0.989, P=0.000) \quad (6)$$

The results showed that in Laoshan, the fluoropolymer manufacturing sources FL2 contributed 46.9% to the $\sum_{13}$PFASs, followed by the metal plating and electrochemical sources (36.3%, FL3), the metal electroplating and electrochemical sources (16.8%, FL1) the material intermediates preparation and fluoropolymer processing aids. The 100% (25.6 pg/m^3) of the observed $\sum_{13}$PFASs was explained by PCA-MLR model.These three sources represented the average concentration contributions of 4.3, 12.0 and 9.6 pg/m^3 to the $\sum_{13}$PFASs, respectively (Table S9). In Xisha Islands, the textile treatment sources FX1 contributed 53.4% to the $\sum_{12}$PFASs, followed by the precious metals sources (42.2%, FX2), the metal electroplating and electrochemical sources (4.39%, FX3), which could indicate that long-distance transport of PFASs from northeastern areas may be a main source of PFASs in Xisha Islands atmosphere. The 100% (8.56 pg/m^3) of the observed $\sum_{12}$PFASs was explained by PCA-MLR model. These three sources represented the average concentration contributions of 4.57, 3.70 and 0.38 pg/m^3 to the $\sum_{12}$PFASs, respectively (Table S10). There were significant differences in the sources of PFASs between Laoshan and Xisha Islands Fig.5. (a), (b). The main sources of PFASs in Laoshan area are fluoropolymer manufacturing and metal electroplating and electrochemistry. The Xisha Islands are mainly based on textile treatment and precious metals, but a small part is still derived from metal plating and electrochemistry. This is due to the industrial structure in different regions.

3.4. Air mass trajectory tracking

The backward trajectory clusters for 24h during the sampling period are shown in Fig.6. (a), (b). In Laoshan, the air masses were transported from all directions. Of these, north (23%), southeast and south (28%+10%) had a relatively high contribution of the total calculated trajectories. In addition, the winds from the north (both northwest and north) and southwest passing through fluorine chemical plants in eastern China and winds from the northeast passing through industrial zones on the Korean Peninsula may exert the influence of PFASs pollution. It was also found that the predominant species of PFAS in the air of Asan Lake area in South Korea was PFOA, accounting for 75.9% of the total (lee et al., 2020), which was consistent with the results of this study. In Xisha Islands, the directions of air masses were generally dominated by the northeast wind, which contributed over 80% of the total calculated trajectories. In addition, a small portion of the air masses was transported from the southeastern over a short or moderate distance. The prevailing directions of air masses transport indicated the potential sources from the open seas. The prevailing direction of air mass transport indicates the potential source from urban industrial areas along the southeast coast and high seas.

Despite geographical separation, the detection of PFAS in Laoshan and Xisha shows a certain degree of similarity, such as PFOA, PFBA, PFDA, PFNA and others. Source apportionment revealed divergent local origins, indicating that their chemical similarity originated from external transport rather than local pollution sources. The dual-source backward trajectory clusters during the 120-hour sampling period at the two locations are shown in Fig.6. (c), (d) . It is consistent with the results of single-source backward trajectory clusters. Combined with real-time meteorological data from Ventusky, demonstrated

https://doi.org/10.5194/egusphere-2025-3127
Preprint. Discussion started: 25 July 2025

overlapping transport paths between the two regions within the same altitude range. Consequently, PFASs migrated from Laoshan to Xisha via atmospheric air mass transport, which synchronized changes in pollutant composition across both areas. This finding revealed the synchronicity of pollutant transport between the two regions and highlighted the potential influence of air mass trajectories on variations in pollutant concentrations.

4. Conclusions

The results demonstrated that legacy PFASs and novel alternatives widely exist in ocean atmosphere, and the main PFASs was PFOA in Laoshan and Xisha Islands. The distribution of PFASs in Xisha Islands atmosphere showed an increasing trend from northeast to southwest, which could be caused by the northeasterly prevailing wind direction. Meanwhile, PCA-MLR models suggested that the three main sources of Laoshan atmospheric were material intermediates preparation and fluoropolymer processing aids sources contributed (16.8%), fluoropolymer manufacturing sources (46.9%), and metal electroplating and electrochemical sources (36.3%), while Xisha Islands were the textile treatment sources contributed (53.4%), precious metals sources (42.2%) and metal electroplating and electrochemical sources (4.39%). The backward trajectory model demonstrated that atmospheric transport to the Laoshan primarily originated from northern, southern, and southeastern, whereas northeastern air masses was the main transport path of the atmosphere in the Xisha Islands. Furthermore, the dual-source trajectory model demonstrated overlapping air mass trajectories between both regions at the same altitude range. Combined with the similarity of PFAS distribution characteristics between the two regions, it revealed that long-distance atmospheric PFAS transport builds Bridges between these geographically different coastal systems.

Data availability

All raw data can be provided by the corresponding authors upon request.

Author contributions

FSH, ZXM, CZH, YTY and YCQ planned the campaign; YTY conducted sample collection; ZXM, and CZH performed the measurements; ZXM, and CZH analyzed the data; ZXM and CZH wrote the manuscript draft; FSH supervised the research and provided intellectual guidance.

Competing interests

The authors declare that they have no conflict of interest

Acknowledgments

This work was supported by the National Natural Science Foundation of China (NSFC 21607018), Chengdu Science and Technology Bureau Key R&D Program (2023-YF09-00013-SN). We thank A/Prof.

https://doi.org/10.5194/egusphere-2025-3127
Preprint. Discussion started: 25 July 2025

Shuhong Fang (Chengdu University of Information Technology) for manuscript refinement guidance and Prof. Caiqing Yan (Shandong University) for sample collection support.

Supplementary data

Supplementary data related to this article can be found in the online version.

References

Ahrens, L., Harner, T., Shoeib, M., Lane, D.A., & Murphy, J.G. 2012. Improved characterization of gas-particle partitioning for per- and polyfluoroalkyl substances in the atmosphere using annular diffusion denuder samplers. Environmental science & technology, 46(13), 7199-7206.

Barber, J.L., Berger, U., Chaemfa, C., Huber, S., Jahnke, A., Temme, C., & Jones, K.C. 2007. Analysis of per- and polyfluorinated alkyl substances in air samples from Northwest Europe. Journal of Environmental Monitoring, 9(6), 530-541.

Billah, M.B. 2016. Determination of perfluorinated compounds (PFCs) in the fine particulate matter (PM2. 5) in China. Jahangirnagar University Journal of Biological Sciences, 5(1), 21-27.

Buck, R.C., Franklin, J., Berger, U., Conder, J.M., Cousins, I.T., de Voogt, P., Jensen, A.A., Kannan, K., Mabury, S.A., & van Leeuwen, S.P. 2011. Perfluoroalkyl and polyfluoroalkyl substances in the environment: terminology, classification, and origins. Integr Environ Assess Manag, 7(4), 513-541.

Cai, M., Yang, H., Xie, Z., Zhao, Z., Wang, F., Lu, Z., Sturm, R., & Ebinghaus, R. 2012. Per- and polyfluoroalkyl substances in snow, lake, surface runoff water and coastal seawater in Fildes Peninsula, King George Island, Antarctica. Journal Of Hazardous Materials, 209-210, 335-342.

Campo, J., Perez, F., Masia, A., Pico, Y., Farre, M., & Barcelo, D. 2015. Perfluoroalkyl substance contamination of the Llobregat River ecosystem (Mediterranean area, NE Spain). Science of the Total Environment, 503-504, 48-57.

Cohen, M.D., Stunder, B.J.B., Rolph, G.D., Draxler, R.R., Stein, A.F., & Ngan, F. 2015. NOAA's HYSPLIT Atmospheric Transport and Dispersion Modeling System. Bulletin of the American Meteorological Society, 96(12), 2059-2077.

Deng, M., Wu, Y., Xu, C., Jin, Y., He, X., Wan, J., Yu, X., Rao, H., & Tu, W. 2018. Multiple approaches to assess the effects of F-53B, a Chinese PFOS alternative, on thyroid endocrine disruption at environmentally relevant concentrations. Science of the Total Environment, 624, 215-224.

Dreyer, A., Kirchgeorg, T., Weinberg, I., & Matthias, V. 2015. Particle-size distribution of airborne poly- and perfluorinated alkyl substances. Chemosphere, 129, 142-149.

Duan, X.L., Zhao, X., Wang, B., Chen, Y., & Cao, S. 2015. Highlights of the Chinese exposure factors handbook. China Environmental Science Press, Beijing, China.

Fang, S., Li, C., Zhu, L., Yin, H., Yang, Y., Ye, Z., & Cousins, I.T. 2019. Spatiotemporal distribution and isomer profiles of perfluoroalkyl acids in airborne particulate matter in Chengdu City, China. Science of the Total Environment, 689, 1235-1243.

Harada, K., Nakanishi, S., Saito, N., Tsutsui, T., & Koizumi, A. 2005. Airborne perfluorooctanoate may be a substantial source contamination in Kyoto area, Japan. Bulletin of Environmental Contamination and Toxicology, 74(1), 64-69.

https://doi.org/10.5194/egusphere-2025-3127
Preprint. Discussion started: 25 July 2025

Hoke, R.A., Ferrell, B.D., Ryan, T., Sloman, T.L., Green, J.W., Nabb, D.L., Mingoia, R., Buck, R.C., & Korzeniowski, S.H. 2015. Aquatic hazard, bioaccumulation and screening risk assessment for 6:2 fluorotelomer sulfonate. Chemosphere, 128, 258-265.

Jiang, Q.T., Lee, T.K., Chen, K., Wong, H.L., Zheng, J.S., Giesy, J.P., Lo, K.K., Yamashita, N., & Lam, P.K. 2005. Human health risk assessment of organochlorines associated with fish consumption in a coastal city in China. Environmental Pollution, 136(1), 155-165.

Kannan, K., Corsolini, S., Falandysz, J., Fillmann, G., Kumar, K.S., Loganathan, B.G., Mohd M, A., Olivero J., Van Wouwe N., & Yang JH. 2004. Perfluorooctanesulfonate and related fluorochemicals in human blood from several countries. Environmental science & technology, 38(17), 4489-4495.

Lai, S., Song, J., Song, T., Huang, Z., Zhang, Y., Zhao, Y., Liu, G., Zheng, J., Mi, W., Tang, J., Zou, S., Ebinghaus, R., & Xie, Z. 2016. Neutral polyfluoroalkyl substances in the atmosphere over the northern South China Sea. Environmental Pollution, 214, 449-455.

Li, Y., Niu, Z., & Zhang, Y. 2022. Occurrence of legacy and emerging poly- and perfluoroalkyl substances in water: A case study in Tianjin (China). Chemosphere, 287(Pt 4), 132409.

Liu, B., Zhang, H., Yao, D., Li, J., Xie, L., Wang, X., Wang, Y., Liu, G., & Yang, B. 2015. Perfluorinated compounds (PFCs) in the atmosphere of Shenzhen, China: Spatial distribution, sources and health risk assessment. Chemosphere, 138, 511-518.

Liu, Z., Lu, Y., Shi, Y., Wang, P., Jones, K., Sweetman, A.J., Johnson, A.C., Zhang, M., Zhou, Y., Lu, X., Su, C., Sarvajayakesavaluc, S., & Khan, K. 2017. Crop bioaccumulation and human exposure of perfluoroalkyl acids through multi-media transport from a mega fluorochemical industrial park, China. Environment international, 106, 37-47.

Prevedouros, K., Cousins, I.T., Buck, R.C., & Korzeniowski, S.H. 2006. Sources, fate and transport of perfluorocarboxylates. Environmental science & technology, 40(1), 32-44.

Qi, Y., He, Z., Huo, S., Zhang, J., Xi, B., & Hu, S. 2017. Source apportionment of perfluoroalkyl substances in surface sediments from lakes in Jiangsu Province, China: Comparison of three receptor models. J Environ Sci (China), 57, 321-328.

Schuetze, A., Heberer, T., Effkemann, S., & Juergensen, S. 2010. Occurrence and assessment of perfluorinated chemicals in wild fish from Northern Germany. Chemosphere, 78(6), 647-652.

Stockholm Convention on Persistent Organic Pollutants (POPs) Annex A&B [Z], UNEP,2019.

Stock, N.L., Lau, F.K., Ellis, D.A., Martin, J.W., Muir, D.C., & Mabury, S.A. 2004. Polyfluorinated telomer alcohols and sulfonamides in the North American troposphere. Environmental science & technology, 38(4), 991-996.

Thurston, G.D., & Spengler, J.D. 1985. A quantitative assessment of source contributions to inhalable particulate matter pollution in metropolitan Boston. Atmospheric Environment 19(1), 9-25.

Wang, Q., Zhao, Z., Ruan, Y., Li, J., Sun, H., & Zhang, G. 2018. Occurrence and distribution of perfluorooctanoic acid (PFOA) and perfluorooctanesulfonic acid (PFOS) in natural forest soils: A nationwide study in China. Science of the Total Environment, 645, 596-602.

Wang, S., Zhao, W., Xu, X., Fang, B., Zhang, Q., Qian, X., Zhang, W., Chen, W., Pu, W., & Wang, X. 2017. Dependence of columnar aerosol size distribution, optical properties, and chemical components on regional transport in Beijing. Atmospheric Environment, 169, 128-139.

Wang, Z., Cousins, I.T., Scheringer, M., Buck, R.C., & Hungerbühler, K. 2014. Global emission inventories for C4 –C14 perfluoroalkyl carboxylic acid (PFCA) homologues from 1951 to 2030, Part I: production and emissions from quantifiable sources. Environment international, 70.

https://doi.org/10.5194/egusphere-2025-3127
Preprint. Discussion started: 25 July 2025

Wang, Z., Cousins, I.T., Scheringer, M., & Hungerbuhler, K. 2013. Fluorinated alternatives to long-chain perfluoroalkyl carboxylic acids (PFCAs), perfluoroalkane sulfonic acids (PFSAs) and their potential precursors. Environment international, 60, 242-248.

Wang Z., Wu T., Duan X., Wang S., Zhang W., Wu X., & Yu Y. 2009. Research on inhalation rate exposure factors of Chinese residents in environmental health risk assessment. Research of Environmental Sciences, 22(10), 1171-1175.

Xiao, F., Halbach, T.R., Simcik, M.F., & Gulliver, J.S. 2012. Input characterization of perfluoroalkyl substances in wastewater treatment plants: source discrimination by exploratory data analysis. Water Research, 46(9), 3101-3109.

Yu, N., Guo, H., Yang, J., Jin, L., Wang, X., Shi, W., Zhang, X., Yu, H., & Wei, S. 2018a. Non-Target and Suspect Screening of Per- and Polyfluoroalkyl Substances in Airborne Particulate Matter in China. Environmental science & technology, 52(15), 8205-8214.

Yu, S., Liu, W., Xu, Y., Zhao, Y., Wang, P., Wang, X., Li, X., Cai, C., Liu, Y., Xiong, G., Tao, S., & Liu, W. 2018b. Characteristics of perfluoroalkyl acids in atmospheric PM10 from the coastal cities of the Bohai and Yellow Seas, Northern China. Environmental Pollution, 243(Pt B), 1894-1903.

Zhang, B., He, Y., Huang, Y., Hong, D., Yao, Y., Wang, L., Sun, W., Yang, B., Huang, X., Song, S., Bai, X., Guo, Y., Zhang, T., & Sun, H. 2020. Novel and legacy poly- and perfluoroalkyl substances (PFASs) in indoor dust from urban, industrial, and e-waste dismantling areas: The emergence of PFAS alternatives in China. Environmental Pollution, 263(Pt A), 114461.

Zhang, T., Sun, H.W., Wu, Q., Zhang, X.Z., Yun, S.H., & Kannan, K. 2010. Perfluorochemicals in meat, eggs and indoor dust in China assessment of sources and pathways of human exposure to perfluorochemicals. Environmental science & technology, 44(9), 3572-3579.

Li, L., Zheng, H., Wang, T., Cai, M., Wang, P., 2018. Perfluoroalkyl acids in surface seawater from the North Pacific to the Arctic Ocean: contamination, distribution and transportation. Environ. Pollut. 238, 168–176.

Sheng, N., Zhou, X., Zheng, F., Pan, Y., Guo, X., Guo, Y., Sun, Y., Dai, J., 2017. Comparative hepatotoxicity of 6: 2 fluorotelomer carboxylic acid and 6: 2 fluorotelomer sulfonic acid, two fluorinated alternatives to long-chain perfluoroalkyl acids, on adult male mice. Arch. Toxicol. 91 (8), 2909–2919.

Zhao, Zhen; Tang, Jianhui; Mi, Lijie; Tian, Chongguo; Zhong, Guangcai; Zhang, Gan; Wang, Shaorui; Li, Qilu; Ebinghaus, Ralf; Xie, Zhiyong; Sun, Hongwen . 2017. Perfluoroalkyl and polyfluoroalkyl substances in the lower atmosphere and surface waters of the Chinese Bohai Sea, Yellow Sea, and Yangtze River estuary. Science of The Total Environment, 599-600, 114–123.

Liu, W., Qin, H., Li, J., Zhang, Q., Zhang, H., Wang, Z., He, X., 2017. Atmospheric chlorinated polyfluoinated ether sulfonate and ionic perfluoroalkyl acids in 2006 to 2014 in Dalian, China. Environ. Toxicol. Chem. 36, 2581–2586.

Young-Min Lee, Ji-Young Lee, Moon-Kyung Kim, Heedeuk Yang, Jung-Eun Lee, Yeongjo Son, Younglim Kho, Kyungho Choi, Kyung-Duk Zoh,2020. Concentration and distribution of per- and polyfluoroalkyl substances (PFAS) in the Asan Lake area of South Korea. Journal of Hazardous Materials,Volume 381, 120909.

Cuihong Qin , Wei Zhang , Zheng Wan. 2021. Research on the Diffusion of Harmful Gases from Ships Based on Gaussian Plume Model. IOP Conference Series: Earth and Environmental Science. 781, 032034

https://doi.org/10.5194/egusphere-2025-3127
Preprint. Discussion started: 25 July 2025

470 Weinberg, I., Dreyer, A., Ebinghaus, R., 2011. Waste water treatment plants as sources of polyfluorinated
471 compounds, polybrominated diphenyl ethers and musk fragrances to ambient air. Environ.
472 Pollut. 159, 125e132.
473 Piekarz A M, Primbs T, Field J A, et al, 2007. Semivolatile fluorinated organic compounds in Asian and
474 western U.S. air masses. Environ Sci Tech, 41: 8248–8255.
475 Gemma Casas, Alícia Martínez-Varela, Jose L. Roscales, Maria Vila-Costa, Jordi Dachs, Begoña
476 Jiménez., 2020. Enrichment of perfluoroalkyl substances in the sea-surface microlayer and sea-
477 spray aerosols in the Southern Ocean, Environmental Pollution, 267, 115512, 0269-7491.
478 Fang X, Wang Q, Zhao Z, et al, 2018. Distribution and dry deposition of alternative and legacy
479 perfluoroalkyl and polyfluoroalkyl substances in the air above the Bohai and Yellow Seas, China.
480 Atmos Environ, 192: 128–135.
481 Yao Y, Chang S, Zhao Y, et al, 2017. Per- and poly-fluoroalkyl substances (PFASs) in the urban, industrial,
482 and background atmosphere of Northeastern China coast around the Bohai Sea: Occurrence,
483 partitioning, and seasonal variation. Atmos Environ, 167: 150–158.
484 Jahnke A, Berger U, Ebinghaus R, et al, 2007. Latitudinal gradient of airborne polyfluorinated alkyl
485 substances in the marine atmosphere between Germany and South Africa (53°N–33°S). Environ
486 Sci Tech, 41: 3055–3061.

https://doi.org/10.5194/egusphere-2025-3127
Preprint. Discussion started: 25 July 2025

Figure captions:

Fig 1. The sampling sites at Laoshan and Xisha Islands, China.

Fig 2. Concentrations of legacy and emerging PFASs in APM of Laoshan (pg/m^3), China.

Fig 3. Concentrations (pg/m^3) and proportion(%) characteristics of PFASs in APM of Xisha Islands, China.

Fig 4. Geographic distribution of PFASs in atmosphere form Xisha Islands including PFOA(a), PFNA(b), the sum of L-PFCAs(C_8-C_{14}) (c) and Σ14PFASs (d).

Fig 5. Sources of PFAS in the atmosphere of Laoshan (a) and Xisha Islands (b), China.

Fig 6. Backward clustering trajectories at the sampling sites of Laoshan (a) and Xisha Islands (b). Dual-source backward clustering trajectories at the sampling sites of Laoshan (c) and Xisha (d) Islands in different time periods.

https://doi.org/10.5194/egusphere-2025-3127
Preprint. Discussion started: 25 July 2025

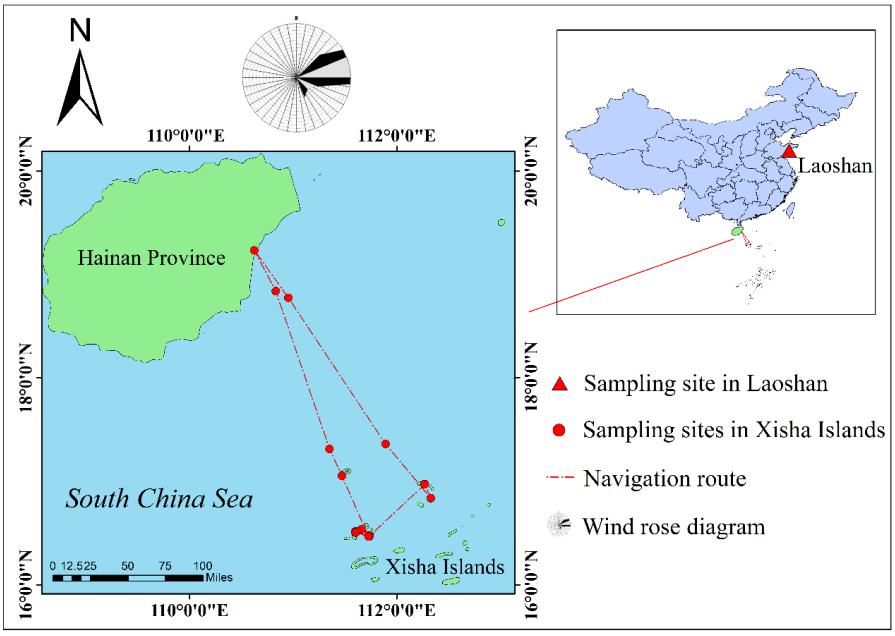

Fig. 1. The sampling sites at Laoshan and Xisha Islands, China

https://doi.org/10.5194/egusphere-2025-3127
Preprint. Discussion started: 25 July 2025

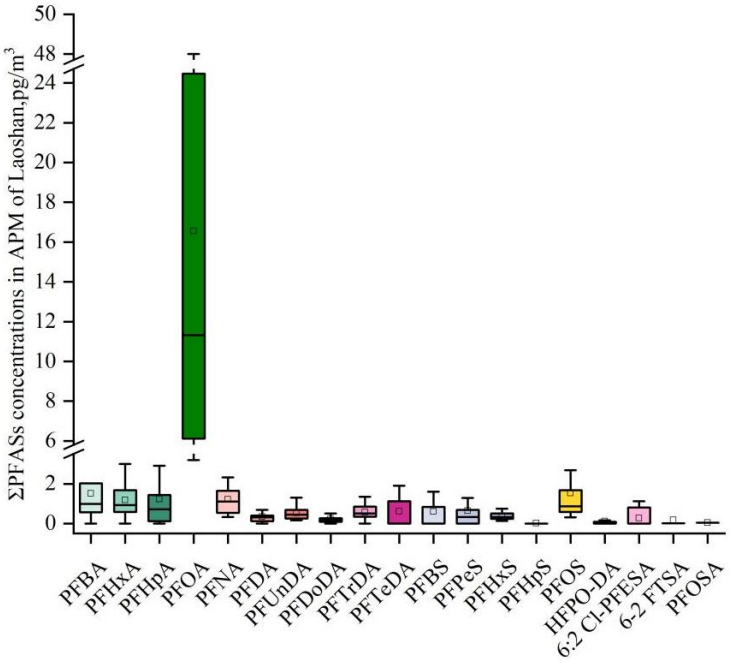

Fig. 2. Concentrations of legacy and emerging PFASs in APM of Laoshan (pg/m^3), China.

https://doi.org/10.5194/egusphere-2025-3127
Preprint. Discussion started: 25 July 2025

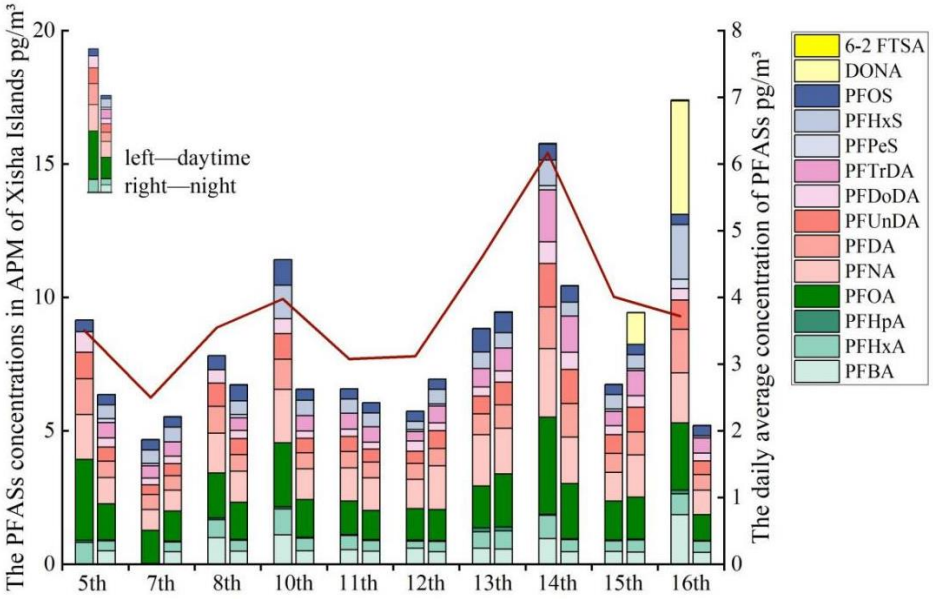

Fig.3. Concentrations (pg/m³) and proportion(%) characteristics of PFASs in APM of Xisha Islands, China.

https://doi.org/10.5194/egusphere-2025-3127
Preprint. Discussion started: 25 July 2025

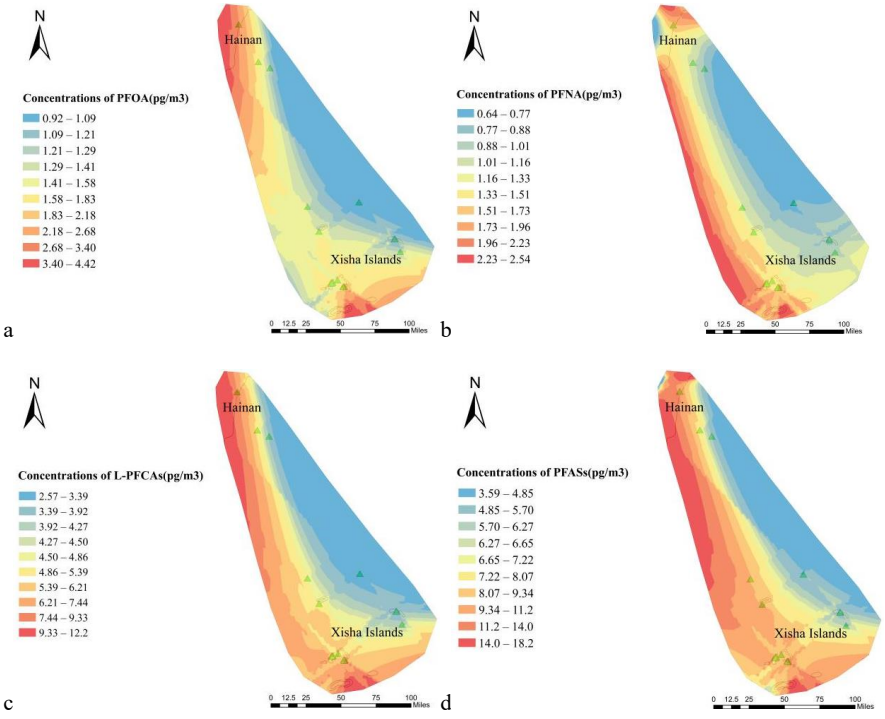

Fig.4. Geographic distribution of PFASs in atmosphere form Xisha Islands including PFOA(a), PFNA(b), the sum of L-PFCAs(C_8-C_{14}) (c) and Σ_{14}PFASs (d).

https://doi.org/10.5194/egusphere-2025-3127
Preprint. Discussion started: 25 July 2025

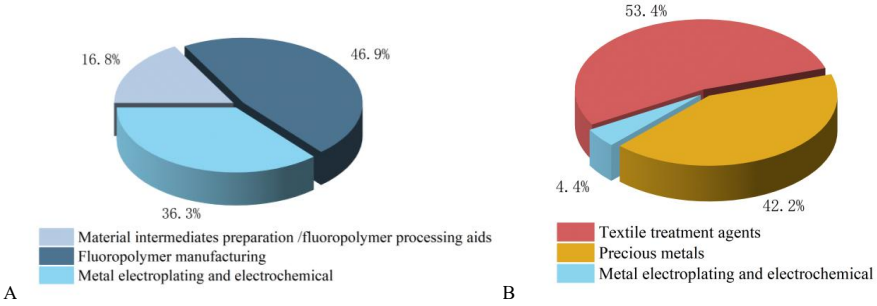

Fig.5. Sources of PFAS in the atmosphere of Laoshan (a) and Xisha Islands (b), China.

https://doi.org/10.5194/egusphere-2025-3127
Preprint. Discussion started: 25 July 2025

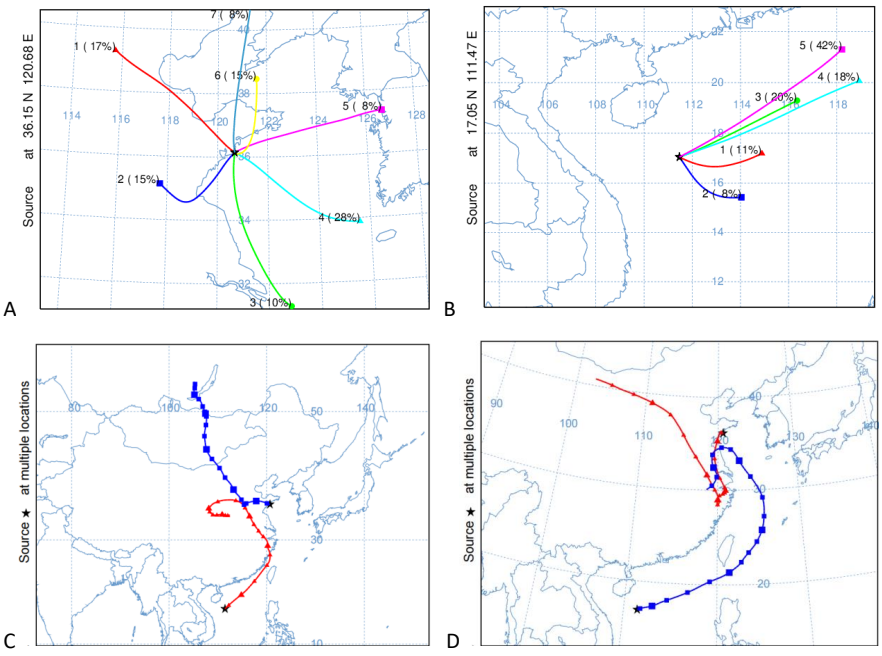

Fig.6. Backward clustering trajectories at the sampling sites of Laoshan(a) and Xisha Islands(b). Dual-source backward clustering trajectories at the sampling sites of Laoshan and Xisha Islands in different sampling time periods including (c) and (d)